Protein Science (1996), 5:1984–1990. Cambridge University Press. Printed in the USA.

The 1.8-Å X-ray structure of the *Escherichia coli* PotD protein complexed with spermidine and the mechanism of polyamine binding

SHIGERU SUGIYAMA,[1] YO MATSUO,[1,4] KATSUMI MAENAKA,[2] DMITRY G. VASSYLYEV,[1] MASAAKI MATSUSHIMA,[1,5] KEIKO KASHIWAGI,[3] KAZUEI IGARASHI,[3] AND KOSUKE MORIKAWA[1]

[1] Protein Engineering Research Institute, 6-2-3 Furuedai, Suita, Osaka 565, Japan
[2] Department of Chemistry & Biotechnology, Faculty of Engineering, Tokyo University, Hongo, Bunkyo-ku, Tokyo 113, Japan
[3] Faculty of Pharmaceutical Sciences, Chiba University, 1-33 Yayoi-cho, Inage-ku, Chiba 263, Japan

(RECEIVED May 7, 1996; ACCEPTED July 2, 1996)

Abstract

The PotD protein from *Escherichia coli* is one of the components of the polyamine transport system present in the periplasm. This component specifically binds either spermidine or putrescine. The crystal structure of the *E. coli* PotD protein complexed with spermidine was solved at 1.8 Å resolution and revealed the detailed substrate-binding mechanism. The structure provided the detailed conformation of the bound spermidine. Furthermore, a water molecule was clearly identified in the binding site lying between the amino-terminal domain and carboxyl-terminal domain. Through this water molecule, the bound spermidine molecule forms two hydrogen bonds with Thr 35 and Ser 211. Another periplasmic component of polyamine transport, the PotF protein, exhibits 35% sequence identity with the PotD protein, and it binds only putrescine, not spermidine. To understand these different substrate specificities, model building of the PotF protein was performed on the basis of the PotD crystal structure. The hypothetical structure suggests that the side chain of Lys 349 in PotF inhibits spermidine binding because of the repulsive forces between its positive charge and spermidine. On the other hand, putrescine could be accommodated into the binding site without any steric hindrance because its molecular size is much smaller than that of spermidine, and the positively charged amino group is relatively distant from Lys 349.

Keywords: bacterial transport system; binding protein; periplasm; polyamine; putrescine; spermidine

Polyamines, such as putrescine, spermidine, and spermine, are linear aliphatic biogenic molecules with two or more positively charged amino groups. They are involved in a wide variety of biological reactions, including nucleic acid and protein synthesis (Tabor & Tabor, 1984; Pegg, 1988).

The polyamine transport genes in *Escherichia coli* have been cloned and characterized (Kashiwagi et al., 1990, 1991, 1992; Furuchi et al., 1991; Pistocchi et al., 1993). The proteins encoded by pPT104 and pPT79 operons constitute the spermidine-preferential and the putrescine-specific uptake system, respectively (Ames, 1986; Furlong et al., 1987). Each polyamine transport system consists of four proteins: pPT104 encodes the PotA, PotB, PotC, and PotD proteins, and pPT79 encodes the PotF, PotG, PotH, and PotI proteins. PotA and PotG are bound to the inner surface of the cytoplasmic membrane. PotB, PotC, PotH, and PotI are transmembrane components that probably form polyamine transport channels. PotD and PotF are periplasmic components. PotD binds both spermidine and putrescine, although spermidine is preferred (Furuchi et al., 1991). In contrast, PotF binds only putrescine (Pistocchi et al., 1993).

The crystal structure of the PotD protein complexed with spermidine was determined previously at 2.5 Å resolution (Sugiyama et al., 1996b). The structure was found to be very similar to those of other periplasmic substrate-binding proteins, such as arabinose (ABP) (Quiocho & Vyas, 1984), galactose/glucose (GGBP) (Vyas et al., 1988), leucine (LBP) (Sack et al., 1989b), leucine/isoleucine/valine (LIVBP) (Sack et al., 1989a), maltodextrin (MBP) (Spurlino et al., 1991; Sharff et al., 1992), sulfate (SBP) (Pflugrath & Quiocho, 1988), and lysine/arginine/ornithine (LAO) (Kang et al., 1991; Oh et al., 1993) binding proteins, with repeating β-α-β units (Quiocho, 1991; Spurlino et al., 1991), although PotD shows no

Reprint requests to: Kosuke Morikawa, Protein Engineering Research Institute, 6-2-3 Furuedai, Suita, Osaka 565, Japan; email: morikawa@beri.co.jp.

[4] Present address: Institute for Social Information Science, Fujitsu Laboratories Ltd., 1-9-3 Nakase, Mihama-ku, Chiba 261, Japan.

[5] Present address: Rational Drug Design Laboratories, 4-1-1 Misato, Matsukawa, Fukushima 960-12, Japan.

significant overall sequence similarity with any of them. In particular, its overall folding topology is the same as those of MBP, SBP, and LAO. The detailed structural comparison has been published elsewhere (Sugiyama et al., 1996b). The 2.5-Å X-ray structure of the PotD–spermidine complex revealed that four acidic residues (Glu 36, Asp 168, Glu 171, and Asp 257) and five aromatic residues (Trp 34, Tyr 37, Trp 255, Tyr 293, and Trp 229) interact with the spermidine molecule. Although the structure of the PotD–putrescine complex remains unknown, mutational analyses suggest that the location of the putrescine molecule bound to PotD is equivalent to that of the diaminobutane moiety of the bound spermidine (Kashiwagi et al., 1996).

In the present study, we have determined the 1.8-Å X-ray structure of the PotD–spermidine complex (Kinemage 1). This detailed structure, refined at higher resolution, reveals the precise mechanism of spermidine binding to PotD, which was not clear in the 2.5-Å structure. To further investigate the differences in the substrate specificity between PotD and PotF, we built a model of the PotF structure, using the PotD structure as a template.

Results and discussion

Crystal structure of the PotD–spermidine complex

In this present work, the PotD–spermidine complex has been crystallized in a tetragonal form. The crystal contained one subunit in an asymmetric unit, whereas the monoclinic form, the structure of which was previously determined at 2.5 Å resolution, contained two dimers in an asymmetric unit (Sugiyama et al., 1996b). The crystal data of the monoclinic and tetragonal forms are summarized in Table 1. The average values of the RMS deviations (RMSDs) between the crystal structures of the monoclinic and tetragonal forms are 0.46 Å for all Cα atoms, 0.43 Å for the amino-terminal domain (N domain) Cα atoms, and 0.47 Å for the carboxyl-terminal domain (C domain) Cα atoms. Although the two crystals have different subunit interactions and molecular arrangements, these RMSDs are very small. This result suggests that the conformations between the N and C domains of PotD–spermidine complex are considerably rigid.

A crystal structure of the PotD–spermidine complex was determined at 1.8 Å resolution (Fig. 1 and Kinemage 1). The PotD molecule is divided into two domains, which are connected through two β strands and one short peptide segment. The two connecting

Table 1. *Crystal data and X-ray data processing statistics*

	Monoclinic form	Tetragonal form
Space group	$P2_1$	$I4_1$
Cell constants (Å)		
a	145.3	130.3
b	69.1	130.3
c	72.5	38.7
β (°)	107.6°	
Resolution (Å)	∞–2.5	∞–1.8
No. of measured reflections	141,071	246,531
No. of independent reflections	40,242	24,579
Completeness (%)	84.4	87.8
R_{merge}[a] (%)	9.4	9.1

[a] $R_{merge} = \Sigma|I - \langle I\rangle|\Sigma\langle I\rangle| \times 100$.

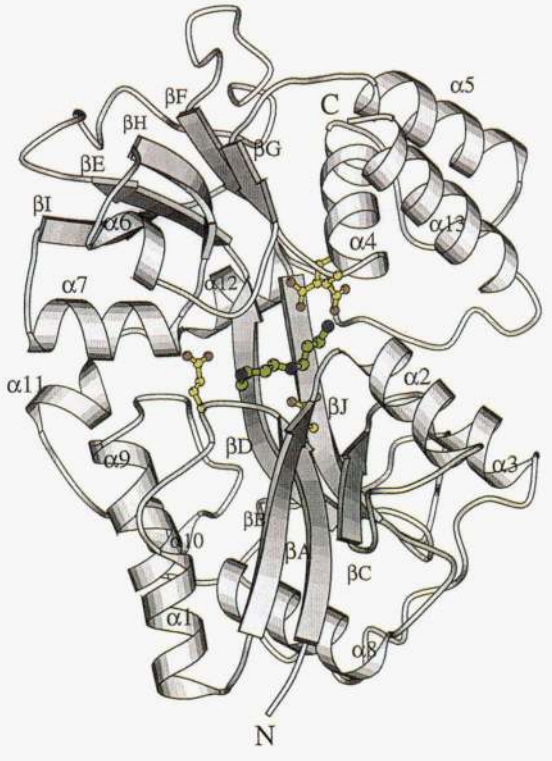

Fig. 1. Overall structure activity and active site of the PotD protein. This ribbon model of the PotD protein was drawn using MOLSCRIPT (Kraulis, 1991). The N domain lies at the bottom and the C domain is at the top. The spermidine molecule is bound in the central cleft between the two domains. Four acidic residues in the active center are indicated by ball and stick models.

strands form a hinge between the two domains, and this hinge lies at the bottom of the cleft. A similar folding pattern is exhibited by the two domains, consisting of a central β sheet and flanking α helices.

The PotD protein exhibits no significant sequence similarity with other periplasmic substrate-binding proteins, such as ABP, GGBP, LBP, LIVBP, MBP, SBP, and LAO (less than 20% sequence identity). However, the PotD protein and these periplasmic proteins share a similar α/β type fold, which consists of repeated β-α-β units. According to the differences in the detailed folding topology, these periplasmic binding proteins can be further classified into two groups, termed I and II (Spurlino et al., 1991). Group I contains ABP, GGBP, LBP, and LIVBP, and Group II includes MBP, SBP, and LAO. Group I has the β-sheet topology of the N domain represented as βn-βD-βC-βA-βB, whereas the topology of group II is βD-βn-βC-βA-βB. In this article, the notation follows that of Spurlino et al. (1991), and βn denotes the β strand that first occurs after the chain returns from the C domain. Therefore, the PotD structure belongs to group II. There is a single substrate-binding site in these periplasmic binding proteins and it lies between the N and C domains. Several structures of these proteins are known with respect to both liganded and unliganded forms, which show that they undergo large hinge-bending motions upon binding ligand. A similar process may occur in the PotD protein (Sugiyama et al., 1996b).

Spermidine binding

The 1.8-Å X-ray structure clearly revealed a water molecule in the substrate-binding cleft of PotD (Kinemage 1). This solvent mol-

Table 2. *Hydrogen bonds and salt bridge interactions between spermidine, protein, and solvent*

Protein/solvent		Spermidine	Distance
Residue	Atom	atom	(Å)
Thr 35	Oγ1	N3	3.3
Glu 36	Oε2	N3	3.1
Tyr 85	OH	N1	2.7
Asp 168	Oδ1	N1	3.7
	Oδ2	N1	3.1
Glu 171	Oε1	N1	2.7
Asp 257	Oδ1	N2	3.5
	Oδ2	N2	2.9
Gln 327	Oε1	N1	2.6
Wat	O	N3	2.7

Protein		Solvent		Distance
Residue	Atom	Residue	Atom	(Å)
Thr 35	Oγ1	Wat	O	3.0
Ser 211	O		O	2.6

ecule, which was not observed in the 2.5-Å monoclinic crystal structure, formed a hydrogen bond with the terminal amino group of the aminobutyl moiety of the spermidine bound to PotD. Furthermore, it formed two hydrogen bonds to the hydroxyl group of Thr 35 and the main-chain carbonyl oxygen of Ser 211. The hydrogen bonds and the salt bridge interactions between the spermidine, protein, and solvent molecules are summarized in Table 2.

These findings are consistent with the results from mutational analyses (Kashiwagi et al., 1996), in which spermidine uptake activities were measured in intact cells expressing mutated PotD proteins. It was found that Glu 171, Trp 255, and Asp 257 participated in the binding of spermidine more strongly than the others among the aforementioned amino acids. Furthermore, the mutant proteins in which Glu 171, Trp 255, and Asp 257 were replaced exhibited lower binding activities for spermidine among the various mutants.

The crystal structure of the free spermidine molecule has already been determined by two groups (Giglio et al., 1966; Huse & Iitaka, 1969). We compared these structures with the 1.8-Å structure of spermidine bound to PotD (Fig. 2). The torsion angles of spermidine trihydrochloride (Giglio et al., 1966), spermidine phosphate trihydrate (Huse & Iitaka, 1969), and spermidine bound to PotD are listed in Table 3. Whereas the backbone conformation of the free spermidine molecule is almost flat, that of the form bound to PotD was bent. This suggests that the spermidine molecule is highly flexible and undergoes a large conformational change when binding to the active site. Distortion of the spermidine conformation is likely to have been caused by the intermolecular contacts with the PotD protein.

Substrate specificity of polyamine-binding proteins

Another *E. coli* periplasmic polyamine binding protein, PotF, exhibits 35% sequence identity to PotD, implying that the overall architectures are well conserved between the two proteins. However, they have different substrate specificities. The PotD protein binds both spermidine and putrescine, with dissociation constants (K_d) of 3.2 μM and 100 μM, respectively (Kashiwagi et al., 1993). On the other hand, PotF binds only putrescine, with a K_d of 2.0 μM (Pistocchi et al., 1993). The present structure, highly refined at 1.8 Å resolution, tempted us to examine how the two proteins could exhibit such different substrate specificities.

The amino acid sequences of the PotD and PotF proteins were compared and aligned (Fig. 3). Among the 14 residues of PotD involved in spermidine binding, 8 of them (Trp 34 with Trp 37, Tyr 37 with Tyr 40, Ser 83 with Ser 85, Glu 171 with Glu 185, Ser 211 with Ser 226, Trp 229 with Trp 244, Asp 257 with Asp 278, Tyr 293 with Tyr 314) are invariant in PotF, and three are replaced by similar amino acids (Thr 35 by Ser 38, Glu 36 by Asp 39, and Trp 255 by Phe 276). Therefore, the different substrate specificity of PotF may be caused mainly by the substitutions at the remaining three residues (Tyr 85 by Ser 87, Asp 168 by Ala 182, and Gln 327 by Lys 349).

The side-chain hydroxyl group of Tyr 85 in PotD was hydrogen bonded to the terminal amino group of the spermidine. Due to the conservation of the hydroxyl side chain, Ser 87 of PotF may retain the hydrogen bond to the spermidine. The carboxyl group of Asp 168 in PotD forms a hydrogen bond and a salt bridge with spermidine. Substitution of Ala 182 may cause PotF to lose this strong electrostatic interaction with spermidine, and hence it decreases its ability to bind spermidine. In the PotD protein, the side

Table 3. *Torsion angles of spermidine molecule*

			Spermidine phosphate trihydrate[b]	
	Spermidine in protein	Spermidine trihydrochloride[a]	Molecule I	Molecule II
N(1)–C(1)–C(2)–C(3)	202.4	180.0	181.8	183.5
C(1)–C(2)–C(3)–N(2)	186.5	180.0	177.3	176.1
C(2)–C(3)–N(2)–C(4)	78.6	180.0	187.5	179.9
C(3)–N(2)–C(4)–C(5)	181.9	180.0	171.9	187.2
N(2)–C(4)–C(5)–C(6)	193.7	180.0	178.5	185.2
C(4)–C(5)–C(6)–C(7)	160.5	180.0	183.9	177.0
C(5)–C(6)–C(7)–N(3)	81.5	180.0	176.9	175.7

[a] Giglio et al. (1966).
[b] Huse and Iitaka (1969).

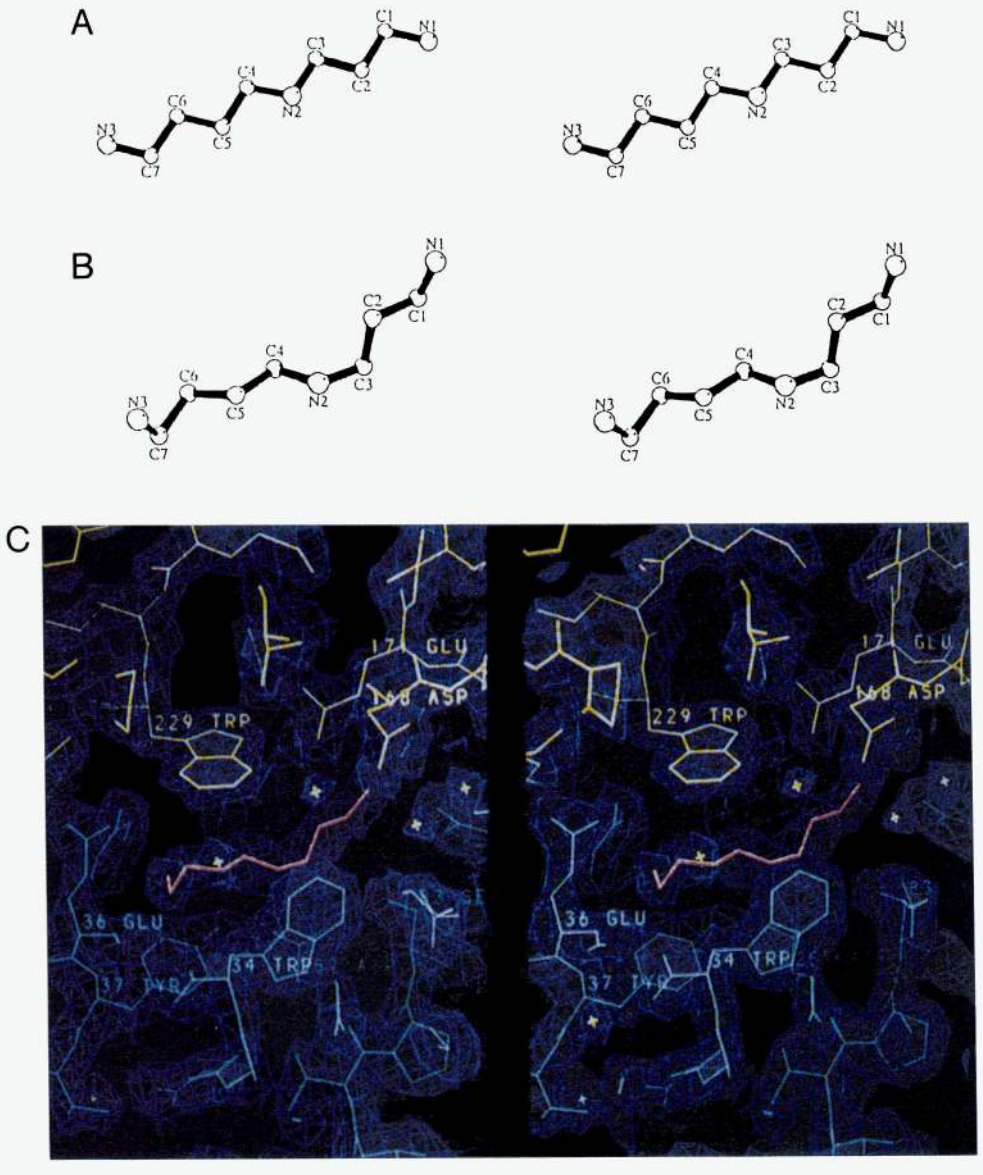

Fig. 2. Stereo drawings of the atomic structures of spermidine molecules. **A:** Spermidine trihydrochloride molecule (Giglio et al., 1966). **B:** The molecule in the tetragonal form of the PotD crystal. **C:** The final $2|F_o| - |F_c|$ electron density around the bound spermidine molecule. Residues of the N domain are green, the C domain is blue, and the substrate is red. A water molecule overlaps with the spermidine molecule on the left side. Through this water molecule, the spermidine molecule forms two hydrogen bonds with Thr 35 and Ser 211.

chain of Gln 327, which is hydrogen bonded to the spermidine amino group, is replaced by Lys 349 in the PotF protein. The positive charge of Lys 349 could cause serious electrostatic repulsion against the positively charged amino group of spermidine, and would thereby greatly reduce the ability of the PotF protein to bind spermidine (Fig. 4).

Putrescine is equivalent to the diaminobutane portion of spermidine, because it lacks the aminopropyl moiety. Mutational analyses indicated that, when bound to PotD, the putrescine molecule occupies the identical position to that of the diaminobutane portion of spermidine bound to PotD (Kashiwagi et al., 1996). It would be reasonable to assume that putrescine could be positioned in PotF in the same manner as found in PotD. The substitutions at the above three positions could therefore disturb spermidine binding by PotF, although they do not affect putrescine binding.

To investigate these implications for binding, a three-dimensional structural model of PotF was constructed, using the 1.8-Å PotD–spermidine complex structure as a template. First, the PotF structure was modeled according to the sequence alignment in the PotD crystal structure. A spermidine molecule was then simply docked into the model, by assuming that it occupies the same position as in the PotD–spermidine complex.

The interaction of spermidine with PotF is shown schematically in Figure 4B. In the model, Asp 39 and Phe 276 can interact with the spermidine molecule. The side-chain hydroxyl group of Ser 87 is 6.49 Å away from the terminal amino group of the aminopropyl portion of the spermidine. This distance is too large for Ser 87 to hydrogen bond to the amino group. The distance between the two amino groups of Lys 349 and spermidine is 1.46 Å, which generates serious steric hindrance.

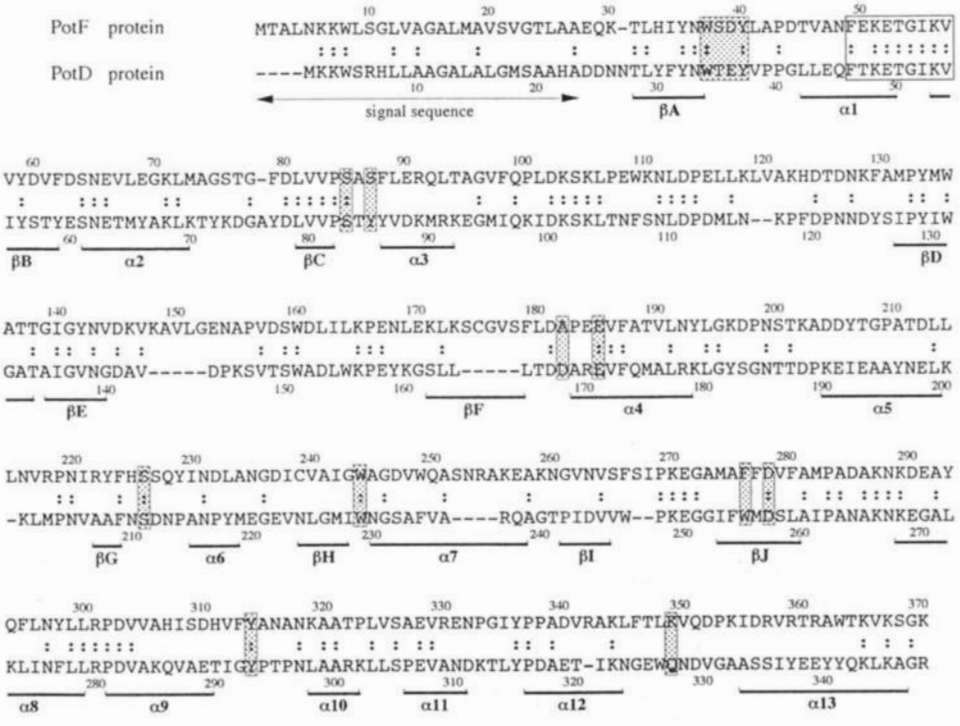

Fig. 3. Sequence alignment between PotD and PotF proteins. Structurally equivalent residues are aligned. The gaps inserted for optimal alignment "-." Pairwise sequence comparison of PotF with PotD exhibited 34% sequence identity. Active residues of PotD and the predicted active residues of PotF are indicated by shaded boxes. A consensus motif region is indicated by a clear box. Fourteen residues of the PotD protein (Trp 34, Thr 35, Glu 36, Tyr 37, Ser 83, Tyr 85, Asp 168, Glu 171, Ser 211, Trp 229, Trp 255, Asp 257, Tyr 293, and Gln 327), which are involved in spermidine binding, are replaced by Trp 37, Ser 38, Asp 39, Tyr 40, Ser 85, Ser 87, Ala 182, Glu 185, Ser 226, Trp 244, Phe 276, Asp 278, Tyr 314, and Lys 349, respectively, in the PotF protein.

In conclusion, the crystal structure of the *E. coli* PotD protein complexed with spermidine was determined at 1.8 Å resolution. The refined structure revealed a water molecule in the binding site of the PotD protein, and through this water molecule, the bound spermidine molecule forms two hydrogen bonds with Thr 35 and Ser 211. In addition to direct polar and van der Waals interactions, these indirect interactions should contribute to spermidine recognition. Furthermore, the PotD structure was found to be very similar to those of MBP, SBP, and LAO, which are members of the periplasmic binding protein superfamily. Structural comparison suggests that a large hinge-bending motion, similar to those observed in these binding proteins, may occur in the PotD protein. The examination, based on the model building, led to the following putative mechanism of polyamine binding by PotF. Putrescine would

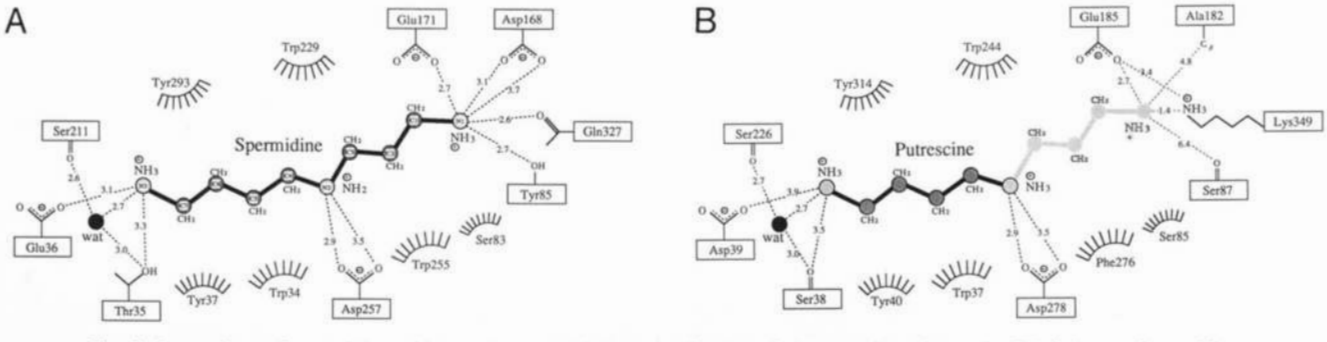

Fig. 4. Interactions of spermidine with protein atoms. Schematic diagram of electrostatic and van der Waals interactions with a polyamine. **A:** The active site of PotD. The methylene backbone of the spermidine makes van der Waals contacts with the aromatic side chains of five residues: Trp 34, Tyr 37, Trp 229, Trp 255, and Tyr 293. All of the three charged amino groups of spermidine make electrostatic interactions with the PotD protein. The terminal amino group of the spermidine aminopropyl moiety forms hydrogen bonds and a salt bridge with the side-chain carboxyl groups of Asp 168 and Glu 171, and is hydrogen bonded to the side chains of Gln 327 and Tyr 85. The amino group in the middle of the spermidine molecule is recognized by the side chain of Asp 257. The other terminal amino group forms hydrogen bonds with the carboxyl side chain of Glu 36 and with the hydroxyl group of the side chain of Thr 35. **B:** Predicted active site of PotF. It is mainly composed of five aromatic side chains, Trp 37, Tyr 40, Trp 244, Phe 276, and Tyr 314.

interact with Trp 37, Ser 38, Asp 39, Tyr 40, Ser 226, Trp 244, Asp 278, and Tyr 314 of PotF. In contrast, PotF does not bind spermidine, particularly because the replacement of Gln 327 of PotD by Lys 349 causes an unfavorable repulsion between the positive charges of its side chain and the terminal amino group of spermidine.

Materials and methods

Crystal structure determination and refinement

The PotD protein was crystallized in two different forms (monoclinic and tetragonal) in the presence of spermidine (Table 1). Procedures for crystallization and data collection were reported previously (Sugiyama et al., 1996a). The cocrystallizations of the PotD protein with spermidine were performed using the sitting drop method. The monoclinic form of PotD complexed with spermidine was obtained at 12 °C in a solution containing 15% (w/v) polyethylene glycol 10,000 and 10 mM Bis-Tris buffer, pH 7.0. The tetragonal form of the same complex was obtained from a crystallization drop containing the protein–spermidine mixture in 15% polyethylene glycol 4,000 and 10 mM HEPES buffer, pH 7.0, at 20 °C. Intensity data were collected, using an automated oscillation camera system (DIP-320, MAC Science) with a cylindrical imaging plate detector, and they were merged by the use of the program PROTEIN, version 3.1 (Steigemann, 1974).

The crystal structure of the tetragonal form was solved using the molecular replacement technique, in which the structure of the monoclinic form refined at 2.5 Å resolution (Sugiyama et al., 1996b) was the search model. Rotation and translation functions were calculated using the X-PLOR program package (Brünger, 1992). A Patterson map for the tetragonal form was calculated using the observed intensities from 15.0 to 4.0 Å resolution. Another Patterson map for search was also calculated from data with the same resolution range, using the initial model in the space group $P1$ lattice, with unit cell dimensions of $a = b = c = 120$ Å. The rotation search based on the PC-refinement procedure (Brünger, 1992) provided one strong peak and the translation search also yielded a prominent peak. Rigid-body and simulated annealing refinements were then conducted with X-PLOR. After these refinements, the R-factor and R-free were reduced from 44.3% to 27.6% and from 43.8% to 36.4%, respectively, for data between 10.0 and 1.8 Å resolution. The $(2|F_o| - |F_c|)$ electron density map showed obvious improvement for all of the protein atoms. The PotD and spermidine molecule could be fitted to the electron density without ambiguity. The refinement was subsequently performed using the programs PROTIN/PROLSQ (Hendrickson, 1985) and CONEXN (Pahler & Hendrickson, 1990). Final R-factor was 19.8% for data from 6.0 to 1.8 Å resolution. Refinement statistics are summarized in Tables 4 and 5. Ramachandran plots for the main-chain torsion angles were analyzed with PROCHECK (Laskowski et al., 1992). All of the ψ and ϕ torsion angles for the non-glycine residues lie within the allowed regions.

Table 4. *Final refinement parameters of the PotD complex (tetragonal form)*

Number of atoms	2,927
Number of solvent atoms	357
Number of spermidine atoms	10
Number of parameters	11,709
Resolution range (Å)	6.0–1.8
Number of used reflections	23,364
R-factor[a] (%)	19.8

[a] $R\text{-factor} = \Sigma||F_o| - |F_c||/\Sigma|F_o| \times 100$.

Table 5. *Weighting parameters in the final refinement of the PotD complex (tetragonal form)*

Restraints	RMSD[a]	Target σ[b]
Distance (Å)		
Bond	0.013	0.020
Angle	0.037	0.035
Planar 1–4	0.046	0.050
Planar groups (Å)	0.011	0.020
Chiral volumes (Å^3)	0.165	0.150
Nonbonded contacts (Å)		
Single torsion	0.186	0.300
Multiple torsion	0.215	0.300
Possible H-bond	0.243	0.300
Torsion angles (°)		
Peptide planar (ω)	1.8	3.0
Staggered (±60 or 180°)	22.3	15.0
Orthogonal (±90°)	32.7	20.0
Isotropic B-factors (Å^2)		
Main-chain bond	1.170	1.500
Main-chain angle	1.866	2.000
Side-chain bond	1.589	2.000
Side-chain angle	2.243	2.500

[a] RMSD from ideality.
[b] The weight for each restraint was $1/\sigma^2$.

Modeling of the PotF structure

The model of the PotF structure was built according to standard homology modeling procedures. The 1.8-Å X-ray structure of PotD was used as a template for the model and alignment of the PotD and PotF sequences was achieved by the method of Needleman and Wunsch (1970), with slight manual modifications. The model was refined by energy minimization using the program PRESTO (Morikami et al., 1992) to remove van der Waals clashes.

Atomic coordinates

Atomic coordinates and the structure factors have been deposited in the Protein Data Bank, Brookhaven National Laboratory, Upton, New York.

Acknowledgments

We thank F. Inoue, S. Hayashi, and M. Ito for computer support. Drs. K. Nishikawa, H. Song, T. Inoue, K. Kurisu, K. Inaka, A. Tomita, and A. Sugimoto are acknowledged for helpful advice and encouragement. We also thank H. Nakamura for valuable advice regarding the homology modeling.

References

Ames GFL. 1986. Bacterial periplasmic transport system: Structure, mechanism, and evolution. *Annu Rev Biochem 55*:397–426.

Brünger AT. 1992. *X-PLOR manual (version 3.1)*. New Haven, Connecticut: Yale University.

Furlong CE. 1987. Osmotic-shock-sensitive transport systems. In: Neidhardt FC, Ingraham JL, Low KB, Magasanik B, Schaechter M, Umbarger HE, eds. *Escherichia coli and Salmonella typhimurium: Cellular and molecular biology*. Washington, DC: American Society for Microbiology. pp 768–796.

Furuchi T, Kashiwagi K, Kobayashi H, Igarashi K. 1991. Characteristics of the gene for a spermidine and putrescine transport system that maps at 15 min on the *Escherichia coli* chromosome. *J Biol Chem 266*:20928–20933.

Giglio E, Liquori AM, Puliti R, Ripamonti A. 1966. The crystal structure of spermidine trihydrochloride. *Acta Crystallogr 20*:683–688.

Hendrickson WA. 1985. Stereochemistry restrained refinement of macromolecular structures. *Methods Enzymol 115*:252–270.

Huse Y, Iitaka Y. 1969. The crystal structure of spermidine phosphate trihydrate. *Acta Crystallogr B 25*:498–509.

Kang CH, Shin WC, Yamagata Y, Gokcen S, Ames GFL, Kim SH. 1991. Crystal structure of the lysine-, arginine-, ornithine-binding protein (LAO) from *Salmonella typhimurium* at 2.7-Å resolution. *J Biol Chem 266*:23893–23899.

Kashiwagi K, Hosokawa N, Furuchi T, Kobayashi H, Sasakawa C, Yoshikawa M, Igarashi K. 1990. Isolation of polyamine transport-deficient mutants of *Escherichia coli* and cloning of the genes for polyamine transport proteins. *J Biol Chem 265*:20893–20897.

Kashiwagi K, Miyamoto S, Nukui E, Kobayashi H, Igarashi K. 1993. Functions of PotA and PotD proteins in spermidine-preferential uptake system in *Escherichia coli*. *J Biol Chem 268*:19358–19363.

Kashiwagi K, Miyamoto S, Suzuki F, Kobayashi H, Igarashi K. 1992. Excretion of putrescine by the putrescine-ornithine antiporter encoded by the *potE* gene of *Escherichia coli*. *Proc Natl Acad Sci USA 89*:4529–4533.

Kashiwagi K, Pistocchi R, Shibuya S, Sugiyama S, Morikawa K, Igarashi K. 1996. Spermidine-preferential uptake system in *Escherichia coli*: Identification of amino acids involved in polyamine binding in PotD protein. *J Biol Chem 271*:12205–12208.

Kashiwagi K, Suzuki T, Suzuki F, Furuchi T, Kobayashi H, Igarashi K. 1991. Coexistence of the genes for putrescine transport protein and ornithine decarboxylase at 16 min on *Escherichia coli* chromosome. *J Biol Chem 266*:20922–20927.

Kraulis PJ. 1991. MOLSCRIPT: A program to produce both detailed and schematic plots of protein structure. *J Appl Crystallogr 24*:946–950.

Laskowski RA, MacArthur MW, Moss DS, Thornton JM. 1992. PROCHECK: A program to check the stereochemical quality of protein structures. *J Appl Crystallogr 26*:283–291.

Morikami K, Nakai T, Kidera A, Saito M, Nakamura H. 1992. PRESTO (PRotein Engineering SimulaTOr): A vectorized molecular mechanics program for biopolymers. *Computers Chem 16*:243–248.

Needleman SB, Wunsch CD. 1970. A general method applicable to the search for similarities in the amino acid sequence of two proteins. *J Mol Biol 48*: 43–453.

Oh BH, Pandit J, Kang CH, Nikaido K, Gokcen S, Ames GFL, Kim SH. 1993. Three-dimensional structure of the periplasmic lysine/arginine/ornithine-binding protein with and without a ligand. *J Mol Biol 268*:11348–11355.

Pahler A, Hendrickson WA. 1990. CONEXN: A procedure to generate ideal groups for stereochemically restrained refinement of protein. *J Appl Crystallogr 23*:218–221.

Pegg AE. 1988. Polyamine metabolism and its importance in neoplastic growth and as a target for chemotherapy. *Cancer Res* 48:759–774.

Pflugrath JW, Quiocho FA. 1988. The 2 Å resolution structure of the sulfate-binding protein involved in active transport in *Salmonella typhimurium*. *J Mol Biol 200*:163–180.

Pistocchi R, Kashiwagi K, Miyamoto S, Nukui E, Sadakata Y, Kobayashi H, Igarashi K. 1993. Characteristics of the operon for a putrescine transport system that maps at 19 minutes on the *Escherichia coli* chromosome. *J Biol Chem 268*:146–152.

Quiocho FA. 1991. Atomic structures and function of periplasmic receptors for active transport and chemotaxis. *Curr Opin Struct Biol 1*:922–933.

Quiocho FA, Vyas NK. 1984. Novel stereospecificity of the L-arabinose-binding protein. *Nature 310*:381–386.

Sack JS, Saper MA, Quiocho FA. 1989a. Periplasmic binding protein structure and function: Refined X-ray structures of the leucine/isoleucine/valine-binding protein and its complex with leucine. *J Mol Biol 206*:171–191.

Sack JS, Trakhanov SD, Tsigannik IH, Quiocho FA. 1989b. Structure of the L-leucine-binding protein refined at 2.4 Å resolution and comparison with the Leu/Ile/Val-binding protein structure. *J Mol Biol 206*:193–207.

Sharff AJ, Rodseth LE, Spurlino JC, Quiocho FA. 1992. Crystallographic evidence of a large ligand-induced hinge-twist motion between the two domains of the maltodextrin binding protein involved in active transport and chemotaxis. *Biochemistry 31*:10657–10663.

Spurlino JC, Lu GY, Quiocho FA. 1991. The 2.3-Å resolution structure of the maltose- or maltodextrin-binding protein, a primary receptor of bacterial active transport and chemotaxis. *J Biol Chem 266*:5202–5219.

Steigemann W. 1974. Die entwicklung und anwendung von rechenverfahren und rechenprogrammen zur structuranalyse von protein am beispel des trypsin-trypsininhibitor komplexes, des frelen inhibitors und der L-asparaginase. [thesis]. München: Technishe Universität.

Sugiyama S, Matsushima M, Saisho T, Kashiwagi K, Igarashi K, Morikawa K. 1996a. Crystallization and preliminary X-ray analysis of the primary receptor (PotD) of the polyamine transport system in *Escherichia coli*. *Acta Crystallogr D 52*:416–418.

Sugiyama S, Vassylyev DG, Matsushima T, Kashiwagi K, Igarashi K, Morikawa K. 1996b. Crystal structure of PotD, the primary receptor of the polyamine transport system in *Escherichia coli*. *J Biol Chem 271*:9519–9525.

Tabor CW, Tabor H. 1984. Polyamines. *Annu Rev Biochem 53*:749–790.

Vyas NK, Vyas MN, Quiocho FA. 1988. Sugar and signal-transducer binding sites of the *Escherichia coli* galactose chemoreceptor protein. *Science 242*:1290–1295.